Available online at www.sciencedirect.com
ScienceDirect
C. R. Physique 9 (2008) 668–680
COMPTES RENDUS PHYSIQUE
http://france.elsevier.com/direct/COMREN/

Synchrotron x-rays and condensed matter/Rayonnement X synchrotron et matière condensée

X-Ray Photon Correlation Spectroscopy at the European X-Ray Free-Electron Laser (XFEL) facility

Gerhard Grübel

Hasylab/DESY, Notkestrasse 85, 22607 Hamburg, Germany

Available online 7 November 2007

Abstract

The proposed European X-ray Free-Electron Laser source (XFEL) will provide extremely brilliant ($B > 10^{33}$ ph/s/mm^2/mrad^2/0.1% bw) and highly coherent X-ray beams. Due to the pulse structure and the unprecedented brightness one will be able for the first time to study fast dynamics in the time domain, thus giving direct access to the dynamic response function $S(Q,t)$, instead of $S(Q,\omega)$, which is of central importance for a variety of phenomena such as fast non-equilibrium dynamics. X-ray Photon Correlation Spectroscopy (XPCS) measures the temporal changes in a speckle pattern produced when coherent light is scattered by a disordered system and therefore allows the measurement of $S(Q,t)$. This article summarizes important aspects of the scientific case for an XPCS instrument at the planned XFEL. New XPCS setups taking account of the XFEL pulse structure are described. ***To cite this article: G. Grübel, C. R. Physique 9 (2008).***

Résumé

Spectroscopie de corrélation de photons X (XPCS) à l'installation européenne de laser aux électrons libres (XFEL). La source européenne laser de rayons X aux électrons libres (XFEL) proposée fournira un faisceau de rayons X extrêmement brillant ($B > 10^{33}$ ph/s/mm^2/mrad^2/0.1% bw) et cohérent. Grâce à la structure pulsée et à la forte brillance du faisceau, il sera possible d'étudier pour la première fois des dynamiques très rapides dans le domaine temporel. Ainsi, la fonction temporelle dynamique $S(Q,t)$ sera directement accessible ce qui est d'une importance capitale pour de nombreux phénomènes tels que les dynamiques rapides hors-équilibres. Comme la spectroscopie de corrélation de photons X (XPCS) permet de mesurer au cours du temps les figures d'interférences de la lumière diffusée, obtenues avec un faisceau cohérent et un système désordonné, $S(Q,t)$ peut être immédiatement déduite avec cette technique. Cet article résume les aspects scientifiques importants pour la construction d'un instrument XPCS dans le cadre du projet XFEL ; les nouveaux dispositifs d'XPCS prenant en compte la structure pulsée de l'XFEL seront en particulier décrits. ***Pour citer cet article : G. Grübel, C. R. Physique 9 (2008).***

Keywords: X-ray Photon Correlation Spectroscopy (XPCS); X-ray Free Electron Laser (XFEL); X-ray speckles; Time-domain dynamics

Mots-clés : Spectroscopie de corrélation de photons X ; Laser de rayons X aux électrons libres ; Figures d'interférences

E-mail address: gerhard.gruebel@desy.de.

1631-0705/$ – see front matter
doi:10.1016/j.crhy.2007.04.006

1. Introduction

Nanoscale dynamics is an omnipresent phenomenon which is investigated at the frontier of condensed matter research. It comprises a multitude of collective processes, such as the visco-elastic flow in liquids, polymer dynamics, protein folding, crystalline phase transitions, glass dynamics or the switching of domains. The time-scales involved range from femtoseconds to seconds. Slow processes ($t > 1$ microsecond) are, in favourable cases, accessible via conventional X-ray Photon Correlation Spectroscopy (XPCS) at 3rd generation synchrotron radiation sources. The study of fast ($t \ll 1$ microsecond) dynamics at large momentum transfers Q is however restricted up to now to energy domain (inelastic) techniques. This, however, will change with the new FEL sources providing extremely brilliant ($B > 10^{33}$ ph/s/mm^2/mrad^2/0.1% bw) and highly coherent X-ray beams [1]. For the first time one will be able to study fast dynamics in the time domain, thus giving direct access to the dynamic response function $S(Q,t)$, instead of $S(Q,\omega)$, which is of central importance for a variety of phenomena such as fast non-equilibrium dynamics initiated e.g. by a short pump pulse.

XPCS measures the temporal changes in speckle patterns produced when coherent light is scattered by a disordered system. At today's 3rd generation synchrotron light sources it can measure the low frequency dynamics (10^6 Hz to 10^{-3} Hz) in a Q range from typically 10^{-3} Å^{-1} up to several Å^{-1} [2]. X-ray photon correlation spectroscopy is in particular complementary to Dynamic Light Scattering (DLS) or Photon Correlation Spectroscopy (PCS) with visible coherent light which also probes slow dynamics ($\omega < 10^6$ Hz) but can cover only the long wavelength $Q < 10^{-3}$Å^{-1} regime. XPCS is furthermore not subject to multiple scattering, a phenomenon frequently complicating the analysis of PCS data in optically opaque systems. Neutron based techniques (inelastic and quasi-elastic neutron scattering, neutron spin-echo) or inelastic X-ray Scattering (IXS), on the other hand, can access the same Q range as storage ring based XPCS but probe the dynamic properties of matter at high frequencies from typically 10^{14} Hz down to about 10^8 Hz. The XFEL with its coherent flux increased by at least 9 orders of magnitude will allow us, for the first time, to cover dynamics up to about 10^{13} Hz at large Q. This is illustrated in Fig. 1, which shows the frequency–wavevector space covered by a selection of relevant methods. Key features of the XFEL source are summarized in Section 2. Relevant problems to be addressed and a selection of prominent examples are summarized in the experimental programme in Section 3. New XPCS techniques are discussed in Section 4. Section 5 summarizes key parameters for a necessary fast 2-D detector system. The requirements and layouts of XPCS instruments at an XFEL are presented in Section 6. A summary and conclusion is given in the last section.

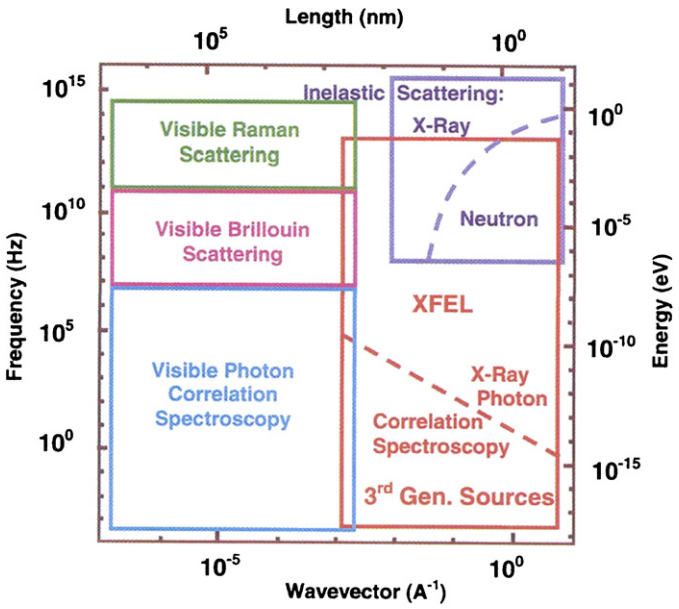

Fig. 1. Frequency–wavevector space covered by different experimental techniques. X-Ray Photon Correlation Spectroscopy (XPCS) can operate at large Q and cover slow dynamics at 3rd Generation Sources and fast dynamics at XFEL sources.

2. The XFEL source

The European X-ray Free-Electron Laser (XFEL) [3] is based on a 1.6 km long superconducting linear accelerator (LINAC). Electron bunches are extracted from a solid cathode by a laser beam, focused and accelerated by an electron RF gun and directed towards the LINAC with 120 MeV energy. The 116 accelerator modules of the LINAC raise the electron energy to 20 GeV. Essential components of the structure are two bunch compressors with the purpose of shortening the bunch length to about 55 μm, which corresponds to a duration of less than 200 fs. A schematic lay-out of the accelerator complex is shown in Fig. 2.

The XFEL LINAC can produce 10 RF pulses per second, each of 600 μs duration, and each pulse can accelerate a train of up to 3000 electron bunches, i.e. with a minimum spacing of 200 ns between successive bunches. Long (100–200 m) undulators will produce ultra-intense and ultra-short pulses of radiation via the Self Amplified Spontaneous Emission (SASE) process. This process starts up from noise and involves micro-bunching at X-ray wavelength of the short electron pulses, thus ensuring the emission processes of the individual electrons in the microbunches are in phase and coherent.

An overview of the main XFEL parameters is given in Table 1. The undulator parameters have been optimised for 0.1 nm wavelength at a beam energy of 17.5 GeV.

The European XFEL Facility in the present design will, in its phase-I, have 5 undulator beamlines, three of which are SASE-FELs (two for the 0.1 nm wavelength regime, one for softer X-rays), the other two for hard X-ray spontaneous radiation. Fig. 3 shows a schematic layout of the electron and photon beam layout. The time structure of the machine is illustrated in Fig. 4.

Initially, ten experimental stations are foreseen. The underground hall has a floor space of 42×85 m^2 available for installation of experimental stations and depending on the layout and space requirements of the experiments, it is conceivable that more stations can be added later. At least one experimental station is expected to be dedicated to coherence based techniques, such as Imaging and/or XPCS. A corresponding experimental program is sketched in Fig. 3

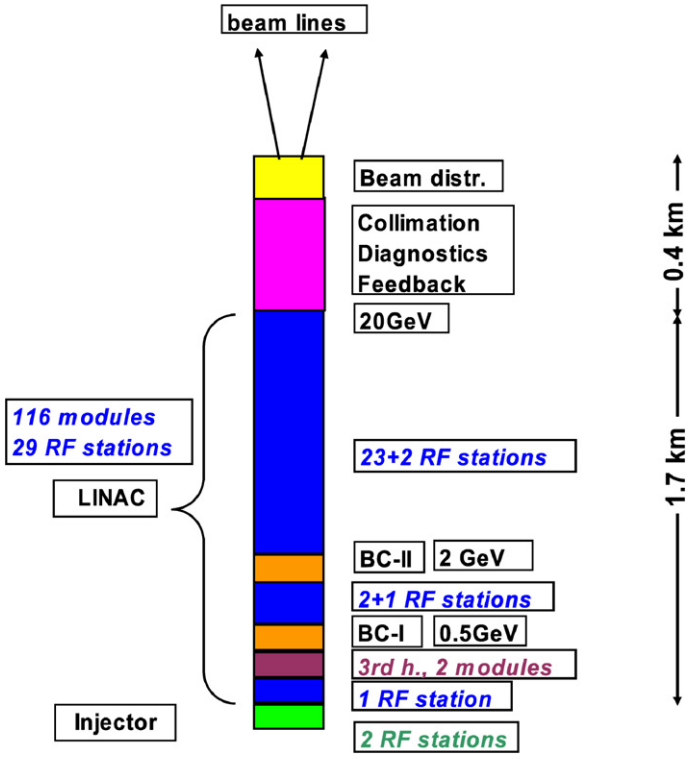

Fig. 2. Basic layout of the XFEL accelerator.

Table 1
XFEL design parameters

Performance goals for the electron beam	
Beam energy range	10–20 GeV
Emittance (norm.)	1.4 mrad mm
Bunch charge	1 nC
Bunch length (1σ)	80 fs
Energy-spread (uncorrelated)	<2.5 MeV rms
Main LINAC	
Acc. gradient @ 20 GeV	23 MV/m
LINAC length	approx. 1.5 km
Average beam current	32.5 μA
Beam pulse length	0.60 ms
No. bunches per pulse (max)	3000
Bunch spacing (min)	200 ns
Repetition rate	10 Hz
Avg. beam power (max)	650 kW
Performance goals for SASE FEL radiation	
Photon energy	15–0.2 keV
Wavelength	0.08–6.4 nm
Peak power	20–150 GW
Average power	40–80 W
Number photons per pulse	$1–300 \times 10^{12}$
Peak brilliance	$5–0.1 \times 10^{33}$ [a]
Average brilliance	$1.6–0.03 \times 10^{25}$ [a]

[a] In units of photons/(s mrad^2 mm^2 0.1% bw).

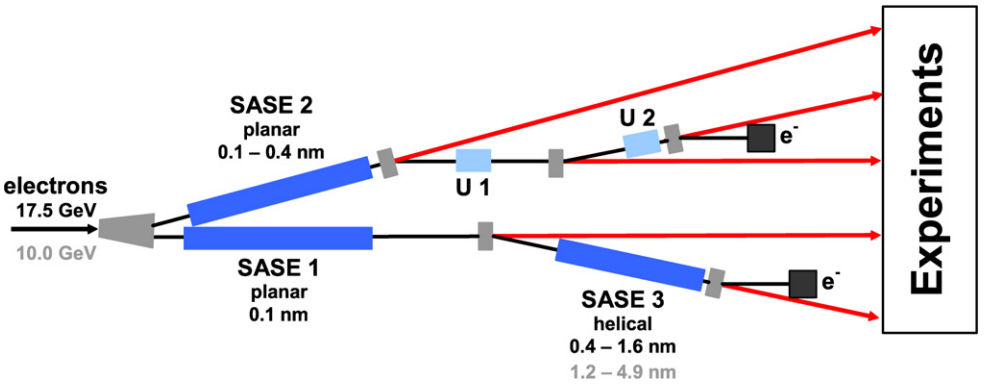

Fig. 3. Schematic view of the branching of electron (black) and photon (red) beamlines through the different SASE and spontaneous emission undulators. Electron beamlines terminate into the two beam dumps, photon beamlines into the Experimental Hall.

3. XPCS based experimental program

Relevant problems to be addressed and a selection of prominent examples are summarized in this section. For a general overview see also Refs. [3] and [4].

3.1. Coherence and correlations

Coherence is one of the most prominent features of the novel X-ray Free-Electron Laser sources. A comprehensive understanding of its coherence and correlation properties is not only of fundamental interest but a necessary condition for coherence based experiments. A characterization of the coherence properties is thus mandatory before proceeding to time domain experiments.

The methodology of characterizing coherence properties in terms of correlation functions is theoretically well developed and experimentally established by the optical laser community. We propose to set-up and carry out an

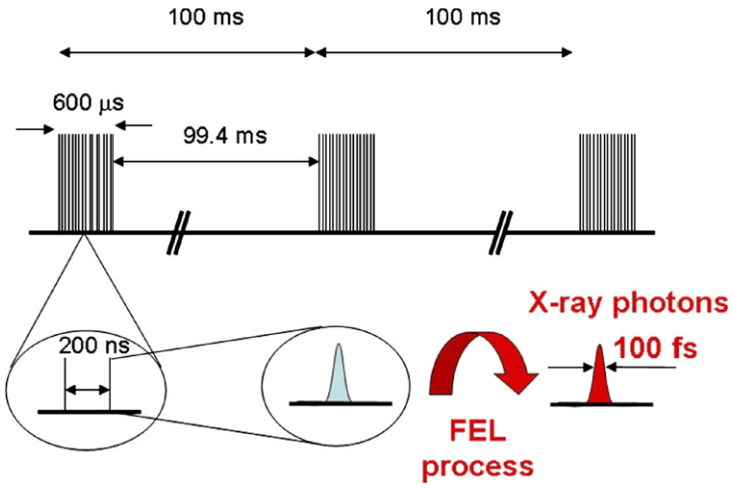

Fig. 4. Time structure of the machine and the photon beam.

experimental programme with the goal to study first- and higher-order correlation functions, which allows one to determine not only the spatial and temporal coherence parameters (including the coherent flux) but also provides insight into the mode structure, photon statistics (bunching/antibunching) and possible non-Gaussian properties of the source. The programme will involve single (100 fs) shot Young's Double Slit experiments and (Hanbury-Brown–Twiss type) intensity-intensity correlation experiments. The results will be fundamental to the tuning and upgrade program of the facility since the results are directly comparable with FEL simulations that predict the mode structure and the degree of coherence. The expected high degree of coherence will also open a route towards non-Gaussian dynamics (e.g. intermittent dynamics in complex fluids [5]) via higher order time correlation functions.

3.2. Study of glassy dynamics

Many liquids, when rapidly cooled below their freezing points, form metastable glassy or amorphous phases. This applies for a wide variety of materials including metallic alloys, oxides such as silica, polymeric materials, and many others. Regardless of their importance, glassy materials are probably among the least understood materials at a fundamental level. Conventional equilibrium statistical mechanics does not predict the existence of the amorphous state, whereas it can explain most other states of matter. Understanding visco-elastic effects in glassy materials is thus an important topic of fundamental research.

Glassy materials can be classified by the nature of their dynamics. In a typical glass-forming system, the viscosity increases exponentially by many orders of magnitude as temperature is lowered, until viscous flow processes are effectively frozen. Methods such as Dynamic Light Scattering (DLS/PCS) or NMR have helped to characterize the relevant relaxation processes such as the primary α relaxation processes with time scales associated with viscosity. Other, faster (β) processes are also observed near the glass transition [6]. The nature and role of these processes are still under debate and discussed e.g. in the framework of mode coupling theory [6,7].

Experiments set up to study the transition require slow rates to look for the underlying thermodynamic phase transition, but need still to be fast enough to avoid crystallization. Light scattering, neutron scattering, and, recently, inelastic X-ray scattering [8] have examined phonon-like modes in these systems and have seen important changes near the glass transition. However measurement times are long, making the systems difficult and frequently even impossible to study with inelastic techniques in particular when the relevant time scales fall below the 1 MHz regime (see also Fig. 1).

XPCS measures the time constants of a system as a function of wave vector and gives direct information on the dynamics. The region of Q and t covered by XPCS is very important for the understanding of the nature of the dynamics in glassforming systems both on the atomic and nanoscale. It is proposed to undertake studies spanning a very large range of time scales (10^{-12} to 10^{3} s) in order to observe the evolution of the dynamics from liquid to

glassy behavior as the temperature is lowered. There are many possible candidates for study, among them systems such as B_2O_3 [9–11].

3.3. Phonon spectroscopy

XPCS can access density fluctuations allowing experiments related to phonon spectroscopy that can be performed today with inelastic X-ray and neutron scattering. However, since the dynamics is measured directly in the time domain, one can access the full time scale from picoseconds to nanoseconds and longer in a single experiment. Moreover, there is the opportunity to examine higher order correlation functions from a cross-correlation analysis of the speckle pattern. While traditional inelastic scattering experiments are limited to density–density correlations, picosecond-XPCS could shine new light on short time dynamics, where coordinated motions of several molecules become important, e.g. during a crystallization process. However, even with the extremely high brilliance of the XFEL, it will be not possible to observe equilibrium dynamics of phonons directly (maybe with the exception of extremely strong acoustic phonons very close to a Bragg peak) since the averaged scattered intensity per speckle will be very low [12]. Therefore one has to add many speckle patterns before a correlation analysis can be done. This will average out random thermal fluctuations. Instead, one will observe phonons that are coherently excited, e.g. by a first X-ray pulse. Typically, a first pulse will generate a hot spot in the sample in the order of the beam size and X-ray attenuation length. A delayed pulse will then reveal insights into the thermal transport processes. To generate a smaller hot spot, a focused laser beam can be also used as a pump. A way to introduce distortions on an even smaller length scale is the use of standing X-ray waves. One could either place the sample in the standing wave field of a Bragg reflection or use X-ray transient grating spectroscopy, where the coherent beam is split up and a standing X-ray pattern is generated by crossing these two beams.

3.4. Surface XPCS with an XFEL

Surface XPCS experiments at 3rd generation storage sources have been performed successfully in the past and surface dynamics has been investigated on a variety of systems, e.g. membranes, polymer films or bulk liquids. Surface XPCS in combination with the X-ray standing wave technique allows one, for example, to study fluctuations of buried interfaces. However, the nanometer length scale of surface dynamics is not accessible due to the limited coherent photon flux. Here the XFEL provides exciting new possibilities. At $Q = 0.1$ Å^{-1} the capillary waves on liquid water are overdamped waves with a correlation function $g_1(t) \sim \exp(-t/t_0)$. Continuum hydrodynamics yields a value of the relaxation time of $t_0 \approx 2.5 \times 10^{-11}$ s which is 100 times longer than the 100 fs pulse width and 10 000 times shorter than the pulse separation of 200 ns. Therefore a delay line unit (see below) is mandatory for measuring relaxation times in this time region.

Assuming a delay line efficiency of 1% one can operate with 2 pulses carrying about 10^{11} photons each. If the detector subtends a solid angle $\Delta\Omega$ the intensity scattered into the detector $I = (\Delta\Omega/A)\ (\mathrm{d}\sigma/\mathrm{d}\Omega)$ can be estimated [13]. Here A describes the beam area and $(\mathrm{d}\sigma/\mathrm{d}\Omega)$ the diffuse scattering cross section. For incident angles below the critical angle of total external reflection the number of photons scattered per (split) XFEL pulse at $Q = 0.1$ Å^{-1} into a detector area of 50×50 μm^2 at 1 m distance is 4×10^{-4}. With 3000 pulses and 10 Hz repetition rate one will detect about 12 photons per second. Thus within minutes sufficient statistics should be obtained. At $Q = 1$ Å^{-1} the count rate is 0.12 ph/s; at $Q = 0.01$ Å^{-1} one finds 1200 ph/s. In the energy domain the overdamped correlation function would yield a Lorentzian energy spectrum centered at $\omega = 0$ with a width ΔE of ca. 20 μeV for $Q = 0.1$ Å^{-1}. This energy broadening would be difficult to resolve with inelastic X-ray scattering. We note that all these experiments are luminosity limited and the given estimates assume in fact the use of all 3000 bunches in a 600 μs bunch train repeated at a 10 Hz repetition rate. Open questions to be further investigated are beam damage and the influence of bulk hydrodynamics [14] at large Q. The onset of non-classical behaviour is a fundamental issue that is of interest for all liquids.

3.5. Time-resolved magnetic scattering

Magnetic X-ray speckle has been observed in a variety of systems [15]. An example for $GdFe_2$ is shown in Fig. 5. More recently it has been shown that magnetic stripe domains can be imaged with a coherent soft X-ray beam [16].

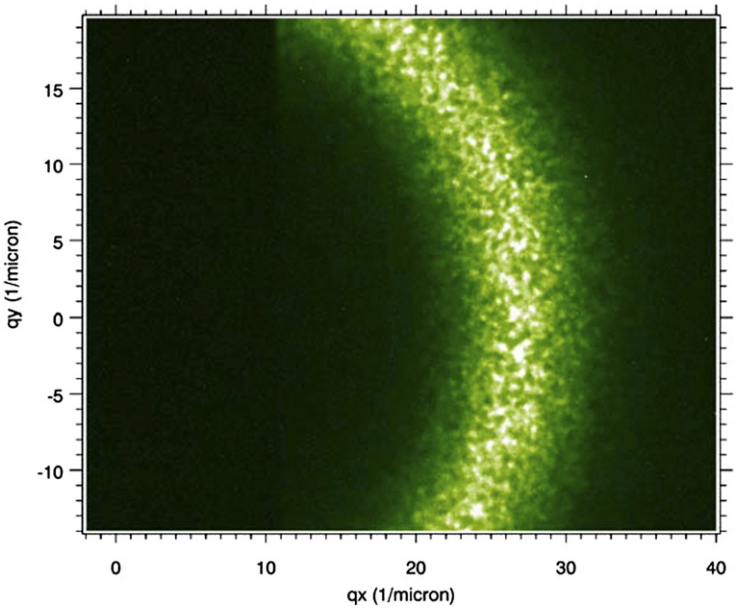

Fig. 5. Magnetic speckle pattern on the first order magnetic diffraction annulus from meandering magnetic stripe domains in a 350 Å thick film of $GdFe_2$ illuminated by a 15 μm diameter beam of circularly polarized X-rays tuned to the Gd M_5 resonance at 1183.6 eV (J.F. Peters et al. [15]).

Sensitivity to magnetism in the CoPt multilayer stemmed from tuning the beam energy to the Co L_3 absorption edge at 778 eV ($\lambda = 15.9$ Å). A reference aperture in the sample allowed the retrieval of the real-space structure of the sample by simple Fourier transform and a resolution of 50 nm was achieved. Provided there is enough intensity, the temporal fluctuations of spins and magnetic domains can be studied by recording the intensity changes at one given point (or Q value) in the scattering pattern as a function of time. Specific to magnetic scattering experiments is the necessity to tune the incident beam energy to distinct absorption edges in the material in order to achieve or increase the sensitivity to the magnetic states or bands. The best suited absorption edges ($M_{4,5}$) in rare earth systems and in 3d transition metals ($L_{2,3}$) would require soft, circularly polarized X-rays as provided by the SASE 3 undulator. As the ultimate size resolution is set by the wavelength of the scattered radiation, XPCS in the soft energy domain will allow the study of domain dynamics down to domain sizes of several nm in 3d transition metals, exploiting 2p-3d scattering resonances, and in rare-earth compounds, exploiting the 3d-4f processes. As the coherent scattering is sensitive to the individual domain pattern, critical dynamics can be probed on a nm length scale down to time scales in the ns and sub-ns range. This opens up new routes to the investigation of domain fluctuations in the vicinity of the (Curie or Néel) transition temperature. Whether or not thin film magnetic system will be able to withstand the full XFEL beam will need to be explored in detail

3.6. Non-equilibrium dynamics

When a disordered homogeneous material is rapidly brought to a new set of conditions, corresponding, for example, to the coexistence of two equilibrium phases, a spatial pattern of domains of the two phases develops. A change of conditions can, for example, be accomplished by a rapid quench from a high temperature to a low one below the miscibility gap. The result of such a quench is the creation of a microstructure of interconnecting domains. These domains grow in order to minimize the areas of the domain walls that separate the phases.

When the average domain size $R(t)$ at time t is large compared to all other relevant length scales except for the dimension L of the system itself, the system looks invariant if all lengths are measured in units of that domain size. The time dependence of the average domain size can typically be described in terms of an exponent n, such that $R \sim t^n$. This scaling hypothesis applies to a large range of systems. For example for systems described by a non-conserved scalar order parameter the growth exponent is found to be $n = 1/2$. This applies, for example, for Ising systems with spin-flip dynamics, binary alloys undergoing an order–disorder transformation or some magnetic materials. In other systems with conserved order parameter and with diffusion being the only growth parameter, one finds $n = 1/3$.

This applies for the conserved Ising model and, e.g., binary alloys undergoing phase separation. Information on the statistics of fluctuations about this average behaviour (which differs from classical fluctuation statistics) is, however, scarce because conventional methods are not easily applicable since (by the nature of the process) the absolute time matters. A time domain method, such as XPCS, can address such processes, as has been shown in recent prototype experiments [17,18]. Here fluctuations about the average intensity can be quantified by means of a two time (t_1, t_2) intensity correlation function

$$C(Q, t_1, t_2) = \left\{\left\langle I(t_1)I(t_2)\right\rangle - \left\langle I(t_1)\right\rangle\left\langle I(t_2)\right\rangle\right\} \Big/ \left|\left\langle I^2(t_1)\right\rangle - \left\langle I(t_1)\right\rangle^2\right|^{1/2}\left|\left\langle I^2(t_2)\right\rangle - \left\langle I(t_2)\right\rangle^2\right|^{1/2}$$

This type of analysis was successfully applied to a borosilicate glass [17]. It was observed that the lagtime $\tau = \Delta t/2$ increases as a function of increasing absolute time t_{mean} thus showing that the dynamics is getting slower as a function of t_{mean}. It was furthermore shown in the experiment that the correlation times actually obey a scaling law in agreement with the model expectations. Similar experiments were carried out in phase-separating AlLi alloys and analyzed successfully in terms of two-time correlation functions [18]. It is evident that the XFEL will allow the study of the early (short time) stages of these processes. The XPCS pump-probe configuration will be ideally suited for any type, but in particular for the study of fast, non-equilibrium processes. One will, for example, be able to study the fluctuations during the nucleation and growth of domains in ferroelectrics after polarization switching as indicated in [19].

4. The XPCS technique

X-ray Photon Correlation Spectroscopy probes the dynamical properties of matter by analyzing the temporal correlations between photons scattered by the material. Correlations of the scattered intensity can be quantified via the normalized time correlation function $g(\tau) = \langle n(t)n(t+\tau)\rangle/\langle n\rangle^2$, where $n(t)$ is the number of detected photons at time t and the brackets denote the time average. XPCS requires the sample to be illuminated coherently. Thus an intense X-ray beam with sufficiently large transverse ξ_t and longitudinal ξ_l coherence length is required. The longitudinal coherence length $(\xi_l) = \lambda \cdot (\lambda/\Delta\lambda)$ depends on the monochromaticity of the beam. With an intrinsic bandwidth of $\approx$0.1% one finds $\xi_l = 100$ nm. Larger longitudinal coherence lengths can be achieved by monochromatization. This estimate of the longitudinal coherence length agrees to within a factor of 2 with the results of simulations for the SASE process that yield a coherence time between 0.2 fs and 0.22 fs for $\lambda = 1$ Å. The longitudinal coherence length must be larger or equal to the maximum path length difference in the sample under investigation. Thus ξ_l sets a limit for the largest accessible momentum transfer Q. The transverse coherence length is usually determined by the source size σ, the wavelength λ and the distance to the source R via $\xi_t \approx (\lambda/2)\ (R/\sigma)$. For the XFEL, the beam can be expected to be largely spatially coherent, and ξ_t corresponds to the beam size. The flux of coherent X-rays is proportional to the source brilliance B via $F_c = (\lambda\ /2)^2 \cdot B$. The impact of the high coherent X-ray flux from the XFEL will be to allow XPCS measurements at higher frequencies ω and on a greater variety of materials, overlapping with energy-domain measurements using neutron and X-ray inelastic scattering. Time-domain XPCS measurements will provide truly complementary information for understanding relaxational processes (e.g. often associated with the 'central peak' in inelastic scattering). The accessible time windows will naturally be influenced by the time structure of the XFEL. To exploit the unique features of the XFEL an instrument with the capability for three types of XPCS techniques was proposed:

- Using the very high time-averaged coherent X-ray flux from the XFEL to carry out XPCS measurements over time scales from 10^{-1} to 10^3 seconds or between 200 ns and 600 μs by recording a sequence of speckle patterns ('Sequential' technique);
- Using the extremely high-peak coherent X-ray flux from the XFEL to carry out XPCS measurements over time scales from 10^{-12} to 10^{-8} seconds using a 'Split-Pulse' technique;
- The 'Pump-Probe' technique is based on a comparison of two speckle patterns, one taken before the pump pulse hits the sample and a second one taken at time Δt after the pump pulse has excited the sample.

4.1. Sequential technique

Important aspects of the microscopic dynamics of systems occur on relatively long time scales, e.g. longer than 10^{-1} s. This means that it will be possible to employ the very high time-averaged coherent X-ray flux from the XFEL,

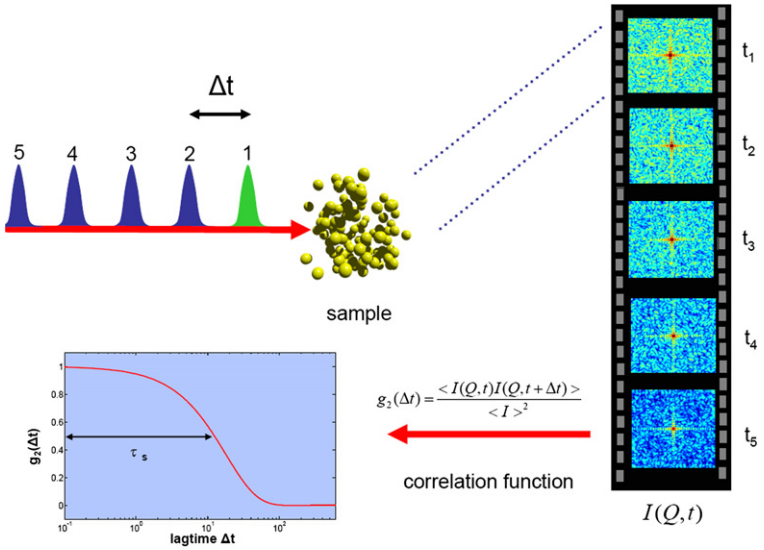

Fig. 6. Illustration of the XPCS sequential technique.

averaged over the 0.1 s repetition rate, to investigate the dynamics using XPCS data collection and analysis techniques that are similar to those used today. Such an experiment consists of collecting a sequence of speckle patterns on an area detector (see Fig. 6). From an analysis of these sequences, correlation times from a few repetition times up to many minutes can be measured. The advantage of the XFEL will be in higher signal rates than currently available. The specific time structure of the XFEL will also allow one to take dynamic data within the 600 μs long macro-bunches. The shortest time will here be given by the micro-bunch separation of 200 ns. It might turn out to be favourable to divide up this time window in logarithmic time bins thus requiring a 2-D detector to operate at 5 MHz frame rate, but with only a limited number of frames to be stored.

4.2. Split-pulse technique

The short pulse duration of the XFEL will allow the extension of XPCS studies to much faster time scales than currently possible. For example, to understand the dynamics in glass-forming systems at the nanoscale, it will be important to carry out studies spanning a very large range of time scales (10^{-12} to 10^{3} s) in order to observe the evolution of the dynamics from liquid to glassy behaviour as the temperature is lowered. In order to probe time scales between 10^{-12} and 10^{-8} s, a Split-Pulse technique (Fig. 7) was proposed [4], taking advantage of the instantaneous brilliance of the XFEL. The concept of the technique is to split each X-ray pulse into two equal-intensity pulses separated in time, but propagating along the same path. The scattering from the two pulses will then be collected during the same exposure of an area detector. If the sample is static on the time scale of the two pulses, then the contrast in the summed speckle pattern will be the same as that from a single pulse. If the sample evolves on this time scale, then the summed speckle pattern will have lower contrast. Thus by analyzing a set of such patterns, each for a different time delay, the correlation times of the system can be measured on time scales down to the pulse duration. A pulse splitter with a path length difference variable from 3×10^{-4} m to 3 m would give delay times from about 10^{-12} to 10^{-8} seconds. Longer time delays between pulses may be possible using two electron bunches in the free electron laser.

4.3. Pump-probe technique

The XPCS pump-probe technique compares two speckle pattern: one before exposing the sample to a pump pulse with a second pattern taken a time interval Δt after the pump pulse. The pump sources for reactions and transformations may comprise optical lasers, the XFEL, a Terahertz source, pulsed electric and magnetic fields, shock waves, and/or others. This allows one to address time scales between 100 fs and typically 200 ns or longer. This configuration can be used to explore the time scales for magnetization processes, phase transitions in ferroelectrics, surface dynam-

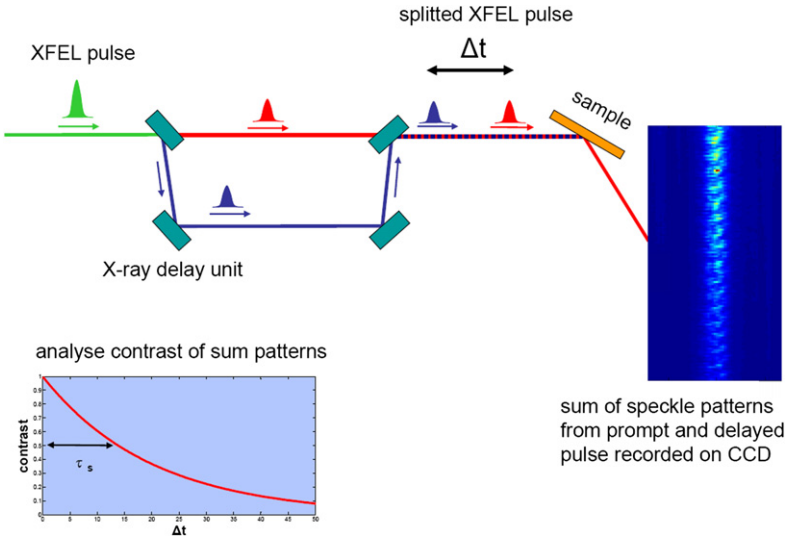

Fig. 7. Illustration of the XPCS split-pulse technique.

ics e.g. during pulsed laser deposition or internal motions in proteins. In principle one could also combine the pump pulse with the above described split-pulse technique.

5. 2-D detectors

The efficient application of the XPCS set-ups described depends crucially upon the availability of 2-D detectors requiring high spatial resolution, high framing rates, high quantum efficiency and low noise. The short pulse duration imposes 'integrating' detectors instead of 'single photon counting systems' while 'single photon sensitivity' at low count rates is required

To achieve maximum contrast, the pixel size D_p must be equal or smaller than the speckle size D_s ($D_p \leqslant D_s$). The *angular* speckle size, θ_s, is given by $\theta_s = \lambda/D_b$ where λ is the wavelength, and D_b the size of the (transversely coherent) beam utilized. D_b can, in principle, be chosen as big as the transverse coherence length ξ_t and since the beam is expected to be spatially fully coherent ξ_t can be as big as the full uncollimated beam. The usable beam size can be limited when it is desired to observe the far-field speckle pattern with a reasonable sample-to-detector distance L. This puts a limit on the incident beam size of $D_b \leqslant (\lambda\ L)^{1/2}$ for a given maximum L. For $\lambda = 1$ Å and $L = 20$ m the beam size should thus not exceed 45 μm. For these parameters the minimum speckle size is $D_s = (\lambda\ L)^{1/2} = 45$ μm, and the required pixel size $D_p \leqslant D_s$. Larger pixel sizes would lead to lower contrast in the speckle pattern.

We see that the smaller the incident beam size, the larger the speckles. However, heat load and sampling volume put a lower limit on the focal spot sizes to be used. A realistic lower limit to the beam size is 25 microns. Using an X-ray wavelength, $\lambda = 1$ Å, we get $\theta_s = 4$ μrad. For a detector distance of 20 m one finds a maximum pixel size of about 80 μm. Taking this as an upper bound one would require angular pixel sizes $(\lambda/L)^{1/2} \leqslant \theta_p \leqslant 4$ μrad.

The detector size needed for the small angle scattering experiment is determined by the minimum length scale one wants to observe. If details down to 10 nm (100 Å) using 1 Å radiation are of interest, one needs to reach a scattering angle of 0.6 degrees. With an angular resolution of 4 μrad, one would need 5000 pixels in each direction. A good strategy is to build a basic building block with 1k × 1k pixels, which will then be tiled to a 5k × 5k imager.

The maximum intensity per pixel per pulse is 1000 photons. Single photon sensitivity is needed at low intensities while one will be counting statistics limited at higher intensities. A base set of requirements for a 2-D detector is summarized in Table 2.

6. Basic requirements for an XPCS instrument

The experiments described above lead to requirements for an instrument for scientific applications using X-ray Photon Correlation (XPCS) spectroscopy techniques. They concern the performance of the light source, of the optical

Table 2
Key parameters for XPCS 2-D detector

	Base requirement	Option
Single photon resolution	yes	–
Photon energy range [keV]	8–12	3–15
Quantum efficiency	>0.8	1
Radiation hardness	yes	–
Harmonics discrimination	no	yes
Number of pixels	1k × 1k	5k × 5k
Need for tiling	yes	–
Preprocessing (hit finding algorithm, autocorrelator, ...)	no	yes
Pixel size [μm]	50–80	⩽50
Vacuum compatibility	no	yes
Signal rate/pixel/bunch	few up to 100	up to 1000
Timing	10 Hz (bunch train)	30 Hz (bunch train)
	5 MHZ during 0.60 ms	–

elements and the diagnostics equipment, of the sample environment and of detectors. The experiments require mostly hard X-ray XFEL radiation at ∼12 keV photon energy. For some experiments one wants to apply 3rd harmonic radiation at considerably higher photon energy, thereby reducing beam damage. For investigations of magnetism tunable radiation around characteristic energies of magnetic materials are of interest. These are the $L_{2,3}$-edges of the transition metals (0.4–1.0 keV) and the $M_{4,5}$-edges of the rare earth elements (0.9–1.5 keV). The full photon energy range of 0.4–12 keV in the fundamental FEL line and ∼30 keV using higher harmonics will not be provided by any of the European XFEL beamlines alone.

To improve the longitudinal coherence, and thereby the accessible Q-range, monochromatization of the incident radiation to the level $\Delta E/E \leqslant 10^{-4}$ needs to be realized. Use of such a monochromator will at the same time increase the observable contrast in the scattering pattern and reduce the beam damage in the sample. For the hard X-ray case double-reflection fixed exit geometry shall be used to maintain flexibility in the setup. The selection of 3rd harmonic radiation shall be achieved as well by this monochromator. In the selection of the optical elements of the monochromators great care has to be taken not to disturb the spatial coherence properties of the XFEL radiation. Crucial for any coherence based technique is the conservation of the X-ray wavefront by the first mirrors and the monochromator. It has been simulated for the hard X-ray case that a figure error in the range of one microradian would distort the beam at the instrument considerably. The target value for the figure error of the mirrors should be substantially better than 0.1 microradians. Whether or not similar stringent requirements also apply for the monochromator crystals is not fully understood yet and a topic of ongoing work. To compensate figure errors resulting from heat load and gravitational sag, the second mirror should have a local active correction mechanism.

The most challenging request for optics comes from the proposed use of X-ray beam splitters for these experiments. A beam-splitter/delay-line unit will comprise up to 8 perfect crystals providing a path length difference between the two split pulses between 1 ps and 10 ns. The beamsize at the sample will be determined by the experiments, in particular the sample geometry. Therefore focusing of the XFEL beam to spot size of the order 10–100 μm should be enabled. The sample to detector distance should be as large as 20 m. Fig. 8 shows a generic layout of an XPCS instrument.

These experiments probe dynamics on the large time scale from 10^{-12} s up to several seconds. This can be achieved by exploiting the sequential and split-pulse techniques proposed in the previous section. The split-pulse and pump-probe techniques make use of the 100 fs pulse duration of the XFEL pulses. Whereas the split-pulse techniques defines its own timescale by using one single pulse, the pump-probe technique uses two different sources and therefore requires synchronization of the two sources. The synchronization should be significantly better than the anticipated time resolution of ∼100 fs. For the same reason the fluctuation of the pulse duration must be small compared to the 100 fs time scale. In addition, a synchronisation of few 100 fs will be required for the operation of X-ray streak cameras.

It is anticipated to use a variety of pulse patterns from single pulses at 10 Hz repetition rate up to several hundreds of X-ray pulses per electron bunch train. A particular request comes from the sequential technique where it is possible

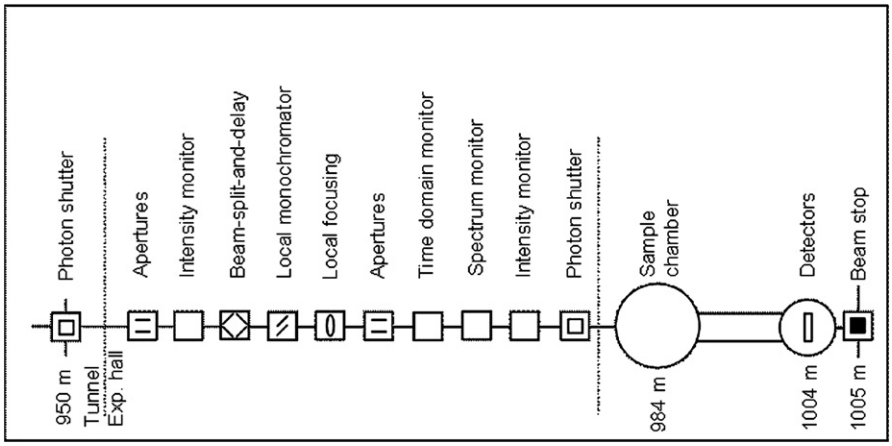

Fig. 8. Schematic layout of an XPCS experimental station.

to use the time pattern of the accelerator to probe time scales from 200 ns (shortest bunch distance) up to 600 μs (duration of bunch train). Adapted detector equipment shall comprise fast point detectors and fast 2-D detector(s). A laser system for pump-probe experiments need to be foreseen.

7. Summary

Essentials of the scientific case for an XPCS instrument at the planned European XFEL source have been described. The instruments will for the first time allow studying fast dynamics in the time domain at nanometer length scales thus giving direct access to the dynamic response function $S(Q,t)$, instead of $S(Q,\omega)$, which is of central importance for a variety of phenomena such as fast non-equilibrium dynamics. There are a variety of scientific questions which can be addressed with the proposed instrument and a few prominent examples have been described. The pulse structure of the XFEL requires the development of new XPCS techniques which has been discussed and illustrated. An outline of the XPCS instruments has been presented.

Acknowledgements

Discussions with and contributions from C. Gutt, H. Sinn, B. Stephenson, T. Tschentscher and A. Duri are acknowledged. Editorial help of S. Grübel is acknowledged.

References

[1] See, for example, G. Grübel, G.B. Stephenson, in: Proceedings of the 4th Generation Light Source Workshop, Advanced Photon Source, Argonne National Laboratory, October 27–29, 1997, and references therein.
[2] S. Brauer, et al., Phys. Rev. Lett. 74 (1995) 2010;
S.B. Dierker, et al., Phys. Rev. Lett. 75 (1995) 449;
T. Thurn-Albrecht, et al., Phys. Rev. Lett. 77 (1996) 5437;
S.G.J. Mochrie, et al., Phys. Rev. Lett. 78 (1997) 1275;
A. Malik, et al., Phys. Rev. Lett. 81 (1998) 5832;
A.C. Price, et al., Phys. Rev. Lett. 82 (1999) 755;
L.B. Lurio, et al., Phys. Rev. Lett. 84 (2000) 785;
D.O. Riese, et al., Phys. Rev. Lett. 85 (2000) 5460;
A. Fera, et al., Phys. Rev. Lett. 85 (2000) 2316;
D. Lumma, et al., Phys. Rev. Lett. 86 (2001) 2042;
I. Sikharulidze, et al., Phys. Rev. Lett. 88 (2002) 115503;
D. Pontoni, et al., Phys. Rev. Lett. 90 (2003) 188301;
H.J. Kim, Phys. Rev. Lett. 90 (2003) 068302;
A. Madsen, et al., Phys. Rev. Lett. 90 (2003) 085701;
C. Gutt, et al., Phys. Rev. Lett. 91 (2003) 076104;

C. Gutt, et al., Phys. Rev. Lett. 91 (2003) 179902 (Erratum);
I. Sikharulidze, et al., Phys. Rev. Lett. 91 (2003) 165504;
A. Madsen, et al., Phys. Rev. Lett. 92 (2004) 096104.
[3] http://tesla.desy.de/new_pages/TDR_CD/PartV/xfel.pdf;
http://tesla.desy.de/new_pages/tdr_update/supplement.html;
XFEL: Technical Design Report, 2006, DESY 2006-097.
[4] LCLS The First Experiments, September 2000;
http://www.www-ssrl.slac.stanford.edu/lcls/papers/lcls.experiments_2.pdf.
[5] L. Cipelletti, L. Ramos, J. Phys. Condens. Matter 17 (2005) R253.
[6] W. Götze, L. Sjogren, Rep. Prog. Phys. 55 (1992) 241.
[7] R. Bergman, et al., Phys. Rev. B 56 (1997) 11619.
[8] M. Grimsditch, M.L. Torell, in: D. Richter (Ed.), Dynamics of Disordered Materials, Springer-Verlag, Berlin, 1989;
M. Russina, et al., Phys. Rev. Lett. 84 (2000) 3620;
U. Buchenau, et al., Phys. Rev. Lett. 77 (1996) 4035;
C. Masciovechio, et al., Phys. Rev. Lett. 80 (1998) 544.
[9] R. Bruning, M. Sutton, Phys. Rev. B 49 (1994) 3124.
[10] A.K. Hassan, et al., Phys. Rev. B 45 (1992) 12797.
[11] D. Engberg, et al., Phys. Rev. B 59 (1999) 4053.
[12] H. Sinn, J. Phys. Condens. Matter 13 (2001) 7525.
[13] S.K. Sinha, et al., Phys. Rev. B 38 (1988) 2297.
[14] S. Mora, J. Daillant, Eur. Phys. J. B 27 (2002) 417.
[15] J.F. Peters, M.A. de Fries, J. Miguel, O. Toulemonde, J. Goedkoop, ESRF Newslett. 15 (2000) 34;
F. Yakhou, A. Letoublon, F. Livet, M. de Boissieu, F. Bley, C. Vettier, ESRF Newslett. 32 (1999) 14;
F. Yakhou, A. Létoublon, F. Livet, M. de Boissieu, F. Bley, J. Magnetism Magnetic Mater. 233 (2001) 119;
K. Chesnel, M. Belakhovsky, F. Livet, S.P. Collins, G. van der Laan, S.S. Dhesi, J.P. Attane, A. Marty, Phys. Rev. Lett. 66 (2002) 172404.
[16] S. Eisebitt, et al., Nature 452 (2004) 885.
[17] A. Malik, et al., Phys. Rev. Lett. 81 (1998) 5832.
[18] F. Livet, et al., Phys. Rev. E 63 (2001) 036108.
[19] A. Grigoriev, D.-H. Do, D.M. Kim, C.-B. Eom, B. Adams, E.M. Dufresne, P.G. Evans, Phys. Rev. Lett. 96 (2006) 187601.